

Change a Bit to save Bytes: Compression for Floating Point Time-Series Data

*

Francesco Taurone, Daniel E. Lucani, Marcell Fehér and Qi Zhang
DIGIT, Department of Electrical and Computer Engineering
Aarhus University
{francesco.taurone, daniel.lucani, sw0rdf1sh, qz}@ece.au.dk

March 9, 2023

Abstract

The number of IoT devices is expected to continue its dramatic growth in the coming years and, with it, a growth in the amount of data to be transmitted, processed and stored. Compression techniques that support analytics directly on the compressed data could pave the way for systems to scale efficiently to these growing demands. This paper proposes two novel methods for pre-processing a stream of floating point data to improve the compression capabilities of various IoT data compressors. In particular, these techniques are shown to be helpful with recent compressors that allow for random access and analytics while maintaining good compression. Our techniques improve compression with reductions up to 80% when allowing for at most 1% of recovery error.

1 Introduction

IoT devices generate large amounts of data that need to be transmitted, stored and analyzed. The advantages of compressing chunks of data include reductions in data transmission costs and more efficient use of bandwidth, as well as reduced data storage. We focus on time-series data compression algorithms [1], where the most common objective is to generate, packetize, compress and store a continuous data stream, it being IoT, financial, or for other use cases, using little memory and computing power.

This paper focuses on data manipulations prior to using a compression algorithm. Our goal is to modify individual samples to make them better suited for compression than the original data stream. More specifically, we propose two novel transforms: the *addition* and *multiplication transform*. We summarize them in Fig. 1, where assuming a one-dimensional set of samples $[x_1, \dots, x_n]$ as input, after applying the transforms, we obtain a dataset $[y_1, \dots, y_n]$. We operate on a per-value basis exploiting floating point representation characteristics, whose basic structure is in Fig. 2, in order to cater to random access compressors, e.g., generalized deduplication [2]. The parameters of each transformation are selected so that all y_i have some identical bits at the same position (e.g., all zero bits in the last 21 mantissa bits in the last row of Table 1). In data recovery, the inverse transformation results in $[\tilde{x}_1, \dots, \tilde{x}_n]$, which is the reconstructed dataset. Although our methods are lossy, the user can specify an upper bound for the maximum recovery error (i.e., distortion) of each sample in the data stream. The larger the maximum allowed error, the more potential for compression.

1.1 Motivating example

Consider that we have two numbers x_1 and x_2 as in Table 1. Although they share a lot of digits in their decimal form, their mantissas have only 2 bits in common. When we first apply the addition

*This work was supported by the IoTalentum Project within the Framework of Marie Skłodowska-Curie Actions Innovative Training Networks (ITN)-European Training Networks (ETN), which is funded by the European Union Horizon 2020 Research and Innovation Program under Grant 953442.

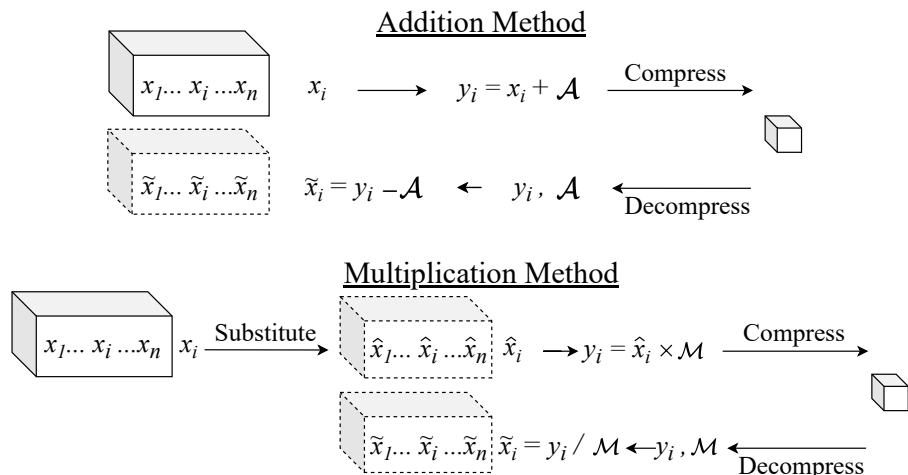


Figure 1: Preprocessing and compression diagram from original x_i to recovered \tilde{x}_i with the two proposed methods. x_i and \tilde{x}_i might differ from each other.

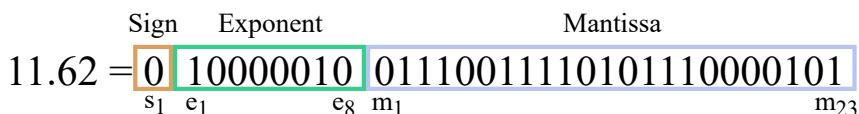


Figure 2: Encoding of a 32-bit IEEE 754 floating point number.

transform, we select a parameter \mathcal{A} to be added to all data in the stream, represented by x_1 and x_2 in this example. Here, we use $\mathcal{A} = 1738.0$, that generates $y_1 = 1791.333$ and $y_2 = 2047.333$. Although the transform seems simple, it results in multiple bits having the same value in both y_1 and y_2 , which can then be compressed more effectively than the originals. Moreover, the exponents of both numbers are now the same as well.

For the multiplication transform, we first modify the bit streams judiciously to create patterns in the mantissa that, when multiplied by a specific \mathcal{M} value, generate a sequence of zeros in the resulting mantissas. The first bit pattern transformation outputs \hat{x}_1 from x_1 and \hat{x}_2 from x_2 . We then multiply by $\mathcal{M} = 3.0$ to generate y_1 and y_2 . We note that all 23 bits in the mantissa are common and could lead to more effective compression.

1.2 Related work

Exploiting data structure and its contextual meaning to achieve compression reductions has been researched extensively, e.g. with images, audio and time-series data [1]. One of the crucial steps for compression is the initial dataset manipulation, where the objective is to clean it and filter out noise, outliers or other unwanted components that might undermine compression. This process is particularly crucial for data coming from IoT devices since sensors can be quite noisy and degrade over time [3]. It is often up to the user's knowledge and experience to prepare data for compression. A complementary approach, usually part of the compressor pipelines, is to represent the same information using predictors or models of the sampled system [4]. Alternatively, we can change the domain of the signal to encode other characteristics, e.g frequency domain in DCT and DWT [5]. Some of these techniques perform well when applied to specific types of dataset, as part of specialized compressors pipelines. We propose two more general-purpose preprocessing methods that transform floating point time-series streams before passing them as input to a wide range of possible compressors. They improve the compressor effectiveness by increasing the number of bit values shared in the dataset to reduce its entropy. This objective is also part of the preprocessing method proposed by Klöwer et al. in *Nature Computational Science* [6], which we use as benchmark for the evaluation of our proposed techniques.

Table 1: Before and after preprocessing

Original	Floating point representation (Sign·Exp·Mant)
$x_1 = 53.333$	$1 \cdot 2^5 \cdot [1. \overbrace{10101010101010101010}^{10} 0100]_{\text{base2}}$
$x_2 = 309.333$	$1 \cdot 2^8 \cdot [1.001 \overbrace{10101010101010101010}^{10} 1]_{\text{base2}}$
<i>Common bits:</i>	xx
Addition transformation, $\mathcal{A} = 1738.0$	
$x_1 + \mathcal{A} = 1791.333$	$1 \cdot 2^{10} \cdot [1.10 \overbrace{11111111}^{10} \overbrace{0101010101010100}^{10}]_{\text{base2}}$
$x_2 + \mathcal{A} = 2047.333$	$1 \cdot 2^{10} \cdot [1.11 \overbrace{11111111}^{10} \overbrace{0101010101010100}^{10}]_{\text{base2}}$
<i>Common bits:</i>	x x xxxxxxxxxxxxxxxxxxxxxxxxxxxxxx
Multiplication transformation, $\mathcal{M} = 3.0$	
$\hat{x}_1 = 53.33333206176758, \hat{x}_2 = 309.3333435058594$	
$\hat{x}_1 \cdot \mathcal{M} = 160.0$	$1 \cdot 2^7 \cdot [1.01 \overbrace{00000000000000000000}^{20}]_{\text{base2}}$
$\hat{x}_2 \cdot \mathcal{M} = 928.0$	$1 \cdot 2^9 \cdot [1.01 \overbrace{00000000000000000000}^{20}]_{\text{base2}}$
<i>Common bits:</i>	xxxxxxxxxxxxxxxxxxxxxxxxxxxxxxxxxxx

2 Background

2.1 Performance metrics

We ultimately want to show that these techniques improve compression performances in terms of output package size. We use the *compression ratio* (CR) as metric, defined as

$$\text{CR} = \frac{\text{size of compressed data}}{\text{size of uncompressed data}}. \quad (1)$$

We also need a parameter called *maximum recovery error*, so the user can impose the recovery error upper bound, which ultimately depends on its application needs. We do so by defining it both in terms of *absolute error*

$$E^\Delta = \max_i \Delta_i \quad \text{with } \Delta_i = |\tilde{x}_i - x_i|, \quad (2)$$

and *relative* to the original value

$$E^\delta = \max_i \delta_i \quad \text{with } \delta_i = \left(\left| \frac{\tilde{x}_i - x_i}{x_i} \right| \right). \quad (3)$$

2.2 Floating point numbers (FP)

While there are various ways to represent real and rational numbers [7], we focus on the standard IEEE-754 [8]. Although our description and experiments use the 32-bit version, the proposed transforms are easily adapted to smaller or extended precision formats in the standard, e.g. 16, 64, and 128 bits. Given a FP number n , its 32-bit structure is divided into three parts, as per Fig. 2:

- *Sign ‘S’*: $\{s_1\}$ bit. ‘0’ for $n \geq 0$, ‘1’ for $n < 0$.
- *Exponent ‘E’*: $\{e_1 \dots e_8\}$ bits. It is biased, meaning that it is interpreted as an unsigned integer once the bias $b = 2^{k-1} - 1 = 127$ is subtracted from it, where k is the number of exponent bits.
- *Mantissa ‘M’*: $\{m_1 \dots m_i \dots m_{23}\}$ bits. Each m_i represents 2^{E-b-i} .

In order to translate bits to numbers, we use the equations

$$\begin{aligned} n &= (-1)^S \cdot 2^{E-b} \cdot (1 + M \cdot 2^{-23}) \\ &= (-1)^S \cdot [2^{E_U} + m_1 \cdot 2^{E_U-1} + \dots + m_{23} \cdot 2^{E_U-23}] \end{aligned} \quad (4)$$

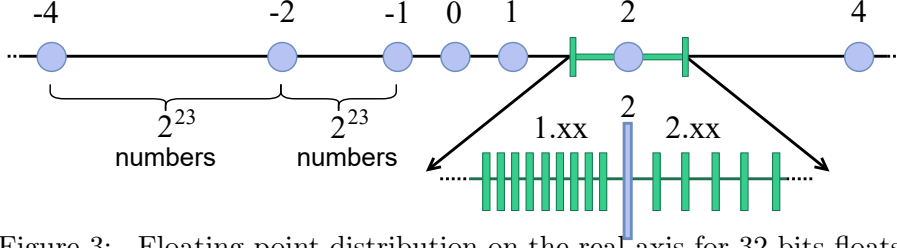


Figure 3: Floating point distribution on the real axis for 32-bit floats.

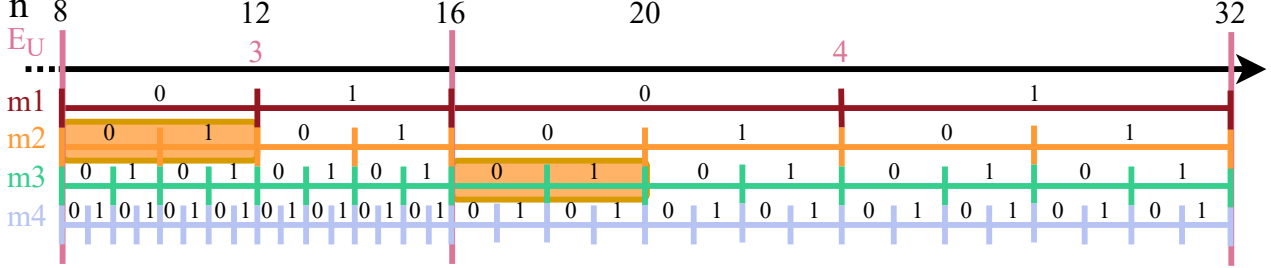


Figure 4: Dataset (range in orange) with $x_i \in [8, 12]$. By applying $y_i = x_i + 8$, we move the dataset to the region $[16, 20]$, where numbers have larger exponent ($E_U = 4$, against the original $E_U = 3$). Therefore, every number in the shifted dataset will have $m_2 = 0$.

where $E_U = E - b \neq 0$. For each n , the smallest quantity we can use in its representation is 2^{E_U-23} , which depends on the exponent of the number. We can define this *Precision* as

$$P(E_U) = 2^{E_U-23}. \quad (5)$$

Therefore, two consecutive FP-representable real numbers in the region with precision $P(E_U)$, differ by $P(E_U)$, or more formally

$$|n_1 - n_2| \geq P(E_U), \forall n_1 \neq n_2 \in [2^{E_U}; 2^{E_U+1}]. \quad (6)$$

Since the distance between two consecutive FP-representable numbers depends on their exponent, i.e. E_U , the further we go from zero, the sparser floating point numbers become on the real axis, as per Fig. 3. When $n \in [0, 2^{-b}[$, with $b = 127$ for 32-bit floats, $E = 0$ and the number is called *subnormal*. The standard defines specific rules for representing and operating with these extremely small and uncommon values, and we will not treat them in the following. The only exception is $n = 0.0$, which is handled separately by the proposed transformations.

3 Preprocessing methods

3.1 Addition transform

This method can be summarized as the following operation:

$$y_i = x_i + \mathcal{A}, \quad \forall x_i \in \mathcal{D} \quad (7)$$

where $\mathcal{A} > 0$ is called *addition parameter*, \mathcal{D} is the dataset. The idea is to shift all samples of the dataset to a suitable region on the real axis. As illustrated in Fig. 4, by strategically choosing \mathcal{A} we can guarantee that all numbers in dataset after the addition transform share the exponent and several mantissa bits. The cost is a possible recovery error due to changing precision from the original region of each sample x_i to the new y_i 's precision. In order to recover the original data, we apply the inverse transformation $\tilde{x}_i = y_i - \mathcal{A}$, thus \mathcal{A} needs to be stored as metadata.

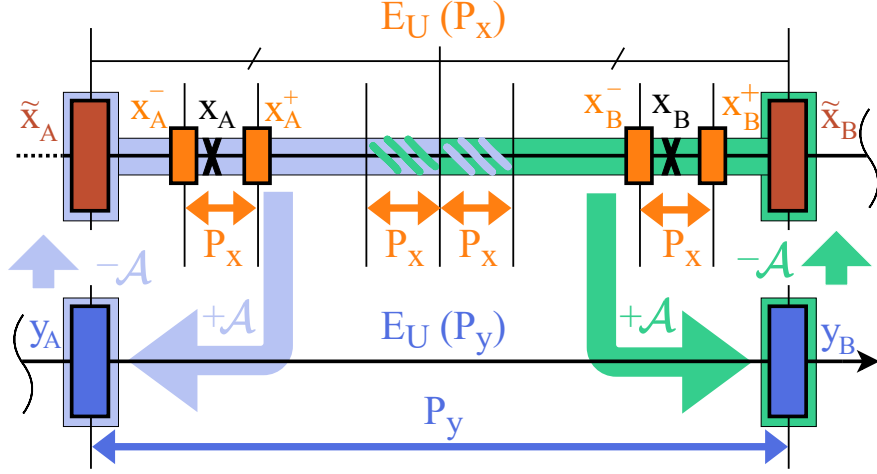


Figure 5: All $x_A \in \mathcal{D}$ in the violet region are transformed to y_A and recovered with \tilde{x}_A . All $x_B \in \mathcal{D}$ in the green region go to y_B and \tilde{x}_B . The result for samples from the region with both colors depends on \mathcal{A} and P_y .

3.1.1 Recovery error

The recovery error occurs when y_i has coarser precision than the original x_i in the dataset. The new precision is shared by all y_i when they have the same E_U (See Fig. 4). The larger the \mathcal{A} value, the more common bits the numbers share and the higher the recovery error. Let us illustrate this with an example. Consider $x_1 = 1.5$ and that $\mathcal{A} = 10^7$. Then, $y_1 = x_1 + \mathcal{A} = 10,000,002$ by adopting the *round to nearest* rounding method from IEEE 754 (three other methods are supported [7]), since the precision of y_1 due to the \mathcal{A} value being used is $P(E_U = 23) = 1.0$. After decompression, the recovered sample will be $\tilde{x}_1 = y_1 - \mathcal{A} = 2.0$ instead of 1.5, generating an absolute error of $\Delta_1 = 2.0 - 1.5 = 0.5$.

Fig. 5 summarizes both the transform and its inverse starting from two real numbers $x_A, x_B \in \mathbb{R}$, to their recovered form \tilde{x}_A and \tilde{x}_B . Considering x_A , we use the rules from IEEE-754 to represent it with a 32 bits FP number and therefore store it as one of its closest neighbour x_A^+, x_A^- in the set of representable FP numbers. Their precision is P_x . With the transform, we reach $y_A = x_A + \mathcal{A}$, having precision P_y . For ensuring more common mantissa bits, we choose \mathcal{A} so that $P_y > P_x$. By applying the inverse transform for recovering the sample, we obtain $\tilde{x}_A = y_A - \mathcal{A}$. Both \tilde{x}_A and \tilde{x}_B belong to the subset of numbers in the P_x region having no component smaller than P_y , since they have at least $\log_2(\frac{P_y}{P_x})$ zeros in the least significant portion of the mantissa. Supposing that all samples after being transformed have the same $E_U(P_y)$, \tilde{x}_A and \tilde{x}_B will be approximating every x_i such that $\tilde{x}_A \leq x_i \leq \tilde{x}_B$. This is because given $x_i \in \mathcal{D}$, during the addition transform $y_i = x_i + \mathcal{A}$, we are losing any info smaller than P_y , and with $\tilde{x}_i = y_i - \mathcal{A}$ we are filling the mantissa bits we lost with zeros. Therefore,

$$\begin{aligned} x_i + \mathcal{A} = y_A, \quad \tilde{x}_A = y_A - \mathcal{A} \quad \forall x_i \in [\tilde{x}_A; \tilde{x}_A + P_y/2 - P_x] \\ x_j + \mathcal{A} = y_B, \quad \tilde{x}_B = y_B - \mathcal{A} \quad \forall x_j \in [\tilde{x}_A + P_y/2 + P_x; \tilde{x}_B] \end{aligned} \quad (8)$$

meaning that different numbers belonging to the same precision region will result in different recovery errors. Due to the standard, y_i and \tilde{x}_i for $x_i \in [\tilde{x}_A + P_y/2 - P_x; \tilde{x}_A + P_y/2 + P_x]$ depend on the rounding method and the selected \mathcal{A} . The use of the addition transform ensures a bound in the recovery error, which is a function of P_y

$$\Delta \leq 2^{E_U^y - 23 - 1} = \frac{P_y}{2}, \quad (9)$$

where E_U^y is the unbiased exponent shared by all samples after the transform.

3.1.2 Selecting the addition parameter

We select \mathcal{A} such that:

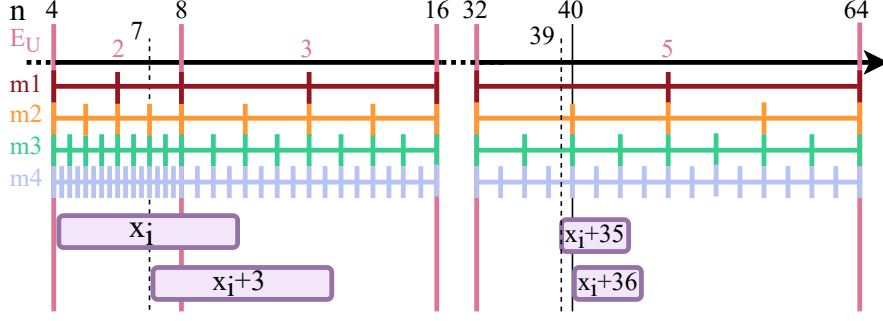


Figure 6: With violet, the dataset range of values. \mathcal{A} should be selected to make all samples share their exponent. Moreover, within the same precision region, some \mathcal{A} result in more common bits than others.

- it is as large as possible while keeping Δ and δ within the user requirements and complying with b) and c);
- the transformed dataset is aligned with the largest powers of 2 in the region;
- it has the same precision of the numbers resulting from the addition with \mathcal{A} .

We can fulfil principle [a.] either by using the error bound in Eq. (2) and Eq. (3) or by checking the real error for each $x_i \in \mathcal{D}$. Since we want all y_i to share the exponent bits as well, we need to select \mathcal{A} so that they lie on a region with equal precision. Considering the example in Fig. 6, by choosing $\mathcal{A} = 3$, $E_U^{y_i} \in [2, 3]$, whereas with $\mathcal{A} = 35$, $E_U^{y_i} = 5 \forall y_i$.

Principle [b.] comes from comparing the choice $\mathcal{A} = 35$ and $\mathcal{A} = 36$ in Fig. 6. Although both shift the dataset to the same exponent region, $\mathcal{A} = 35$ will result in $m_2 \in \{0, 1\}$, whereas with $\mathcal{A} = 36$, $m_2 = 1$, making m_2 shared. The alignment with the powers of 2 within the selected region is key, maximizing common mantissa bits. The larger the power of 2 aligned with the shifted dataset, the more mantissa bits are shared.

Principle [c.] is needed to avoid a counterintuitive phenomenon while selecting \mathcal{A} . Although conventional wisdom would suggest that the smaller we choose \mathcal{A} , the smaller and more precise the transformed numbers in the dataset are, ultimately leading to smaller recovery errors, this is not always the case: it is only true when $x_i + \mathcal{A} \in 2^{E_U^{\mathcal{A}}}$, where $E_U^{\mathcal{A}}$ is \mathcal{A} 's unbiased exponent. By selecting an \mathcal{A} compliant with this last requirement, it is guaranteed that smaller addition parameters always lead to decreasing recovery errors. The implementation used in this paper for choosing \mathcal{A} is

$$\text{Select } \mathcal{A} : \max(x_i \in \mathcal{D}) + \mathcal{A} = 2^{E_U^{\mathcal{A}}+1} - 2^{E_U^{\mathcal{A}}-23}. \quad (10)$$

3.2 Multiplication transform

This method can be summarized as

$$y_i = \hat{x}_i \cdot \mathcal{M}, \quad \hat{x}_i = f(x_i, \mathcal{M}) \quad \forall x_i : x_i \in \mathcal{D} \quad (11)$$

where we call \mathcal{M} the *multiplication parameter*, and f is a function that *substitutes* each data sample x_i in the dataset with \hat{x}_i , a version arbitrarily close to the original, but with the nice property of resulting in many zeros once multiplied by \mathcal{M} . So, in contrast to the addition transform, we apply the multiplication transform on \hat{x}_i rather than on the original x_i . We aim to maximize the number of least significant bits in the mantissa equal to zeros. Let us explain this with an example.

3.2.1 Numerical example

We consider $x_1 = 363.754$ and $x_2 = 366$, with x_2 having 16 consecutive zeros at the end of the mantissa and x_1 having none. In order to increase the number of common ending zeros, we propose substituting x_1 and x_2 with numbers that show the desired zeros after being multiplied by a carefully selected

multiplication parameter \mathcal{M} . We consider $\hat{x}_1 = 363.7894592285156$ and $\hat{x}_2 = 366.03509521484375$ with $\mathcal{M} = 57$. Then, $y_1 = \hat{x}_1 \cdot \mathcal{M} = 20736.0$ and $y_2 = \hat{x}_2 \cdot \mathcal{M} = 20864.0$, which share the last 16 zeros. By storing y_1, y_2 and \mathcal{M} , we can recover the original numbers via the divisions $\tilde{x}_1 = y_1/\mathcal{M} = \hat{x}_1$ and $\tilde{x}_2 = y_2/\mathcal{M} = \hat{x}_2$ with maximum deviation $\delta < 0.01\%$. Other existing methods, like [6], directly approximate x_1 by removing all unwanted least significant mantissa bits to reach 16 ending zeros, where the recovered sample is $\tilde{x}_1 = 362.0$, with deviation $\delta = 0.48\%$.

3.2.2 Selecting the multiplication parameter

We use an approach that maps known values (\mathcal{M}) to known mantissa patterns that result in all zero sequences after their multiplication. A possible way to think about this is the equivalent in base 10. We know that all numbers ending with $.5$, once multiplied by $\mathcal{M} = 2$, finish with $.0$, or that the ending sequence 1.25×8 always results in 0.00 . The same concept applies to floating point multiplication, where patterns expressed in base 2 can be exploited as substitutions for x_i 's mantissas. After $y_i = \hat{x}_i \cdot \mathcal{M}$, all bits in y_i 's mantissa, from the bit representing the starting power of 2 the pattern onward, will be zeros, making the length of the zeros-sequence an arbitrary choice.

Table 2: \mathcal{M} unique patterns in base 2 (with 1 as MSB), expressed in hex

\mathcal{M} Pattern	\mathcal{M} Pattern	\mathcal{M} Pattern	\mathcal{M} Pattern	\mathcal{M} Pattern	\mathcal{M} Pattern	\mathcal{M} Pattern	\mathcal{M} Pattern
3 0x2	11 0x2e8	190x35e50	27 0x25ed0	35 0xea0	43 0x2fa0	51 0xa0	59 0x22b63cbeea4e1a0
5 0xc	13 0x9d8	21 0x30	290x8d3dcb0	370xdd67c8a60	45 0xb60	530x9a90e7d95bc60	610x864b8a7de6d1d60
7 0x4	15 0x8	23 0x590	31 0x10	39 0xd20	470x572620	55 0x94f20	
9 0x38	17 0xf0	250xa3d70	33 0x3e0	41 0xc7ce0	490x14e5e0	57 0x23ee0	

In Table 2, we list the unique patterns for each odd number $\mathcal{M} \in \{3, \dots, 61\}$. The larger \mathcal{M} is, the bigger the product's result and, therefore, the worse its precision, which generally leads to worse recovery errors. The table could be expanded by including for each \mathcal{M} all patterns belonging to its factors, which also produce zeros. We do not consider even \mathcal{M} since powers of 2 in multiplications only affect the exponent, leaving the mantissa intact. Examples of this process are in Table 3, where

Table 3: Examples of base patterns substitutions and multiplications

$x_i = 19.6$	$\mathcal{M} = 13$	Pattern = 000100111011	x_i Mantissa = 00111001100110011001101					
\hat{x}_i	$E_U^{\hat{x}_i}$	Ext	\hat{x}_i Mantissa	y_i	$E_U^{y_i}$	y_i Mantissa	Ending zeros	Δ
19.61538506	4		0011 1001110110001001111	255.0	7	1111111 0000000000000000	16	0.02
19.38461494	4		00 1101100010011110110001	252.0	7	11111 0000000000000000	18	0.22
18.46153831	4		00100111011000100111011	240.0	7	111 0000000000000000	20	1.14
29.53846169	4	001	11011000100111011000101	384.0	8	10000000000000000000	22	9.94
19.69230843	4	0001	00111011000100111011001	256.0	8	00000000000000000000	23	0.09

$x_i \rightarrow \hat{x}_i \rightarrow y_i = \hat{x}_i \cdot \mathcal{M}$. Each pattern instance is boxed. Underlined bits differ from the originals, colored bit in the same row represent equal powers of 2. Ext = mantissa extension: when looking for patches, we can append to the mantissa any number of 0s, followed by a 1.

$x_i = 19.6$ gets substituted in multiple ways using the pattern associated with $\mathcal{M} = 13$. Looking at the first row, suppose that we want to obtain 16 ending zeros from a substitution of 19.6 yet to be found after multiplying by 13 and that our error bound imposes $E_U^{y_i} = 7$. Therefore, the zeros will start from m_8 (in red), which represents the power $2^{7-8} = 2^{-1}$. The bit in x_i that corresponds to the same power is m_5 (in red), and we should start patching from that position onward. We use the bit-shifted version of the pattern minimizing necessary changes to the mantissa (underlined) to limit the error Δ . Here, the pattern needs to be repeated twice (see boxes around the pattern) in order to fill the portion of the mantissa to be patched. After m_{23} , we crop it by rounding to the nearest, producing y_i . From these examples we can conclude that:

- Patterns are bit-shifting invariant.
- Starting patching from the left results in a larger error and more common zeros.
- Typically, the more bits you modify from the original mantissa, the bigger the error will be.
- More zeros at the end of the mantissa do not necessarily mean a larger recovery error.

3.2.3 Scaling up to datasets

So far, we have applied the multiplication transform only to sets of up to 2 numbers, finding many possible substitutions with varying performances. However, we need to process larger collections of numbers, and looking at Fig. 1 we want to find a single \mathcal{M} that suits all x_i and maximizes the number of common ending zeros. In the current implementation, we approach this problem with a brute force search, where first we analyze all $x_i \in \mathcal{D} \forall \mathcal{M} \in [3, 61]$ looking for substitutions that fulfil the error bound. Among these multiplication parameters, we select the one that maximizes the number of common zeros for the dataset. The transformed dataset is then built by substituting each x_i with \hat{x}_i using the substitution corresponding to the chosen \mathcal{M} , having at least the minimum number of ending zeros found in the search and the smallest possible error.

3.2.4 Multiply and check

Due to the *round to nearest* approximation method, there are some numbers \tilde{y}_i that can not have $m_{23} = 0$ when reached via $\tilde{y}_i = \hat{x}_i \cdot \mathcal{M}$. These numbers are off from being all-ending-zeros by P : after the multiplication, we might need to adjust the result with $y_i = \tilde{y}_i \pm P$.

4 Performance evaluation

In order to evaluate the performance of our proposed preprocessing techniques, we compare CR using the setups summarized in Table 4. We analyze the reduction in CR of our proposed addition and

Table 4: Performance evaluation setup

Compressors	Preprocessing	Dataset collection	Example
■ <i>Greedy-GD</i> [9]	○ - Addition transf. with E^Δ and E^δ	aarhus citylab [10]	[35.87]
■ <i>bzip2</i> [11]	▽ - Multiplication transf. with E^Δ and E^δ	chicago [12]	[20.5,0,-0.082,0.055,2,12.7]
■ <i>lz4</i> [13]	× - Info content transf. with E^Δ and E^δ [6]	cbb g2 [14]	[14310,403388]
■ <i>zstd</i> [15]	— - Lossless, it removes decimals by multiplying all samples for a power of 10	cbb dim2 [14]	[12856, 705226]
		uci (<i>3500 samples</i>) [16]	[3.5892]
		cmummac (<i>20000 samples</i>) [17]	[-0.497314,0.425049,-0.036255,-0.755371]

multiplication transforms, against a similar lossy preprocessing technique and a lossless method. The recent work [6] also tries to maximize the number of ending zeros in the mantissa to achieve better compression. It does so by computing the information content of each mantissa bit, rounding to zero the ending mantissa bits below a certain threshold. In order to adapt this algorithm to our error-bound approach, for all dimensions in each dataset, we found the minimum retained information content limit that fulfilled the error condition under analysis. The *lossless preprocessing method* simply eliminates all decimals in the dataset by multiplying all samples with a power of 10.

We use the no-preprocessing results (CR_{NP}) as baseline for comparing performances, with the formula

$$\Delta CR_{\%} = (CR - CR_{NP}) / CR_{NP} \cdot 100. \quad (12)$$

Therefore, $\Delta CR_{\%} < 0$ indicates improved compression. In Fig. 7, on the horizontal axis, we plot the actual maximum error on the recovered dataset imposing the error bounds $E^\Delta \in \{0.01, 0.1, 0.5, 1.0\}$ and $E^\delta \in \{0.01\%, 0.1\%, 0.5\%, 1.0\%\}$. The chosen datasets represent different combinations of datatypes, sizes and number of dimensions: *aarhus citylab* [10] and *uci* [16] for floats with one dimension, *cmummac* [17] for multidimensional floats, *cbb gs* and *cbb dim2* [14] for multidimensional integers and *chicago* [12] for a mix of integers and floats. The compressors we use are *Greedy-GD* [9], a dictionary-based algorithm using deduplication with random access capabilities, as well as three other well-established compressors for comparison, namely *bzip2* [11], *LZ4* [13] and *Zstandard* [15].

The results in Fig. 7 show that our proposed preprocessing methods outperform the one in [6] for all datasets and compressors except in Fig. 7c using E^δ , achieving up to 46% better CR in Fig. 7f. In Fig. 7a and Fig. 7d, the information content transform cannot achieve errors below the desired bounds, leaving the datasets unprocessed with $\Delta CR_{\%} = 0$.

For all datasets and compressors, with $\Delta \leq 1$ or $\delta \leq 1\%$, both addition and multiplication transforms improve compression with respect to the non-preprocessed datasets, with reductions up

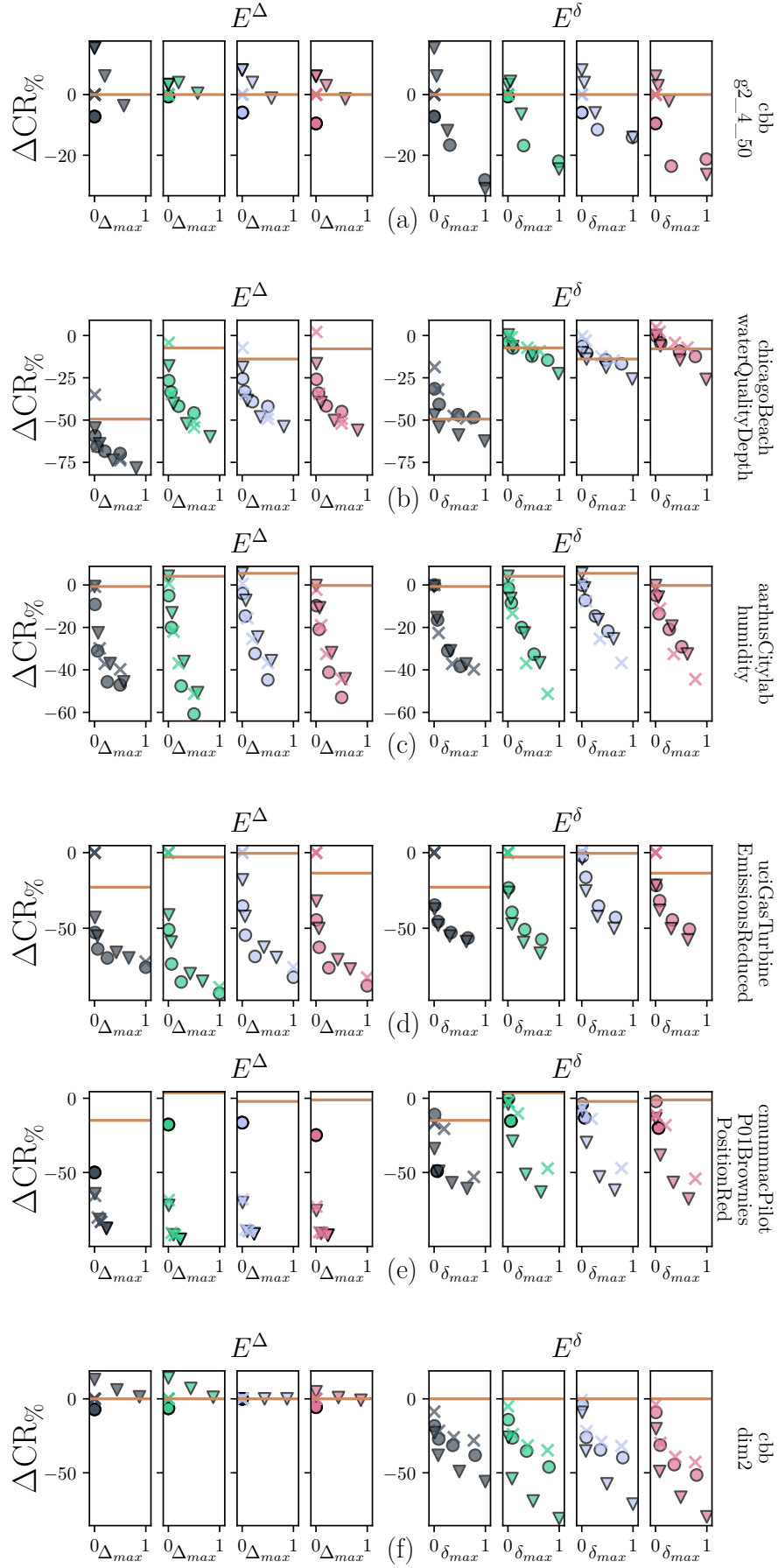


Figure 7: Results to compare the novel preprocessing techniques against the lossy method in [6] (\times) and a lossless (orange line) solution, using an array of error bounds, compressors and datasets. All results are relative to the CR with no preprocessing, which acts as baseline $\Delta\text{CR}_{\%} = 0$.

to 80%. We see cases in Fig. 7a, Fig. 7c and Fig. 7f with E^Δ where for small error bounds the non-preprocessed dataset performs better: however, by switching from E^δ to E^Δ (and vice-versa) or relaxing a bit the error bound, we always achieve improvements.

We also notice that when addition and multiplication transforms outperform the non-preprocessed datasets, they surpass the lossless performances too, represented by the orange line. This line lies on $y = 0$ in Fig. 7a and Fig. 7f since they are integer datasets: the lossless algorithm has no effect on them. As expected, a higher compression can be achieved at the expense of higher recovery errors.

Moreover, the choice between addition and multiplication transform depends on the dataset and the error-bound method. For example, in Fig. 7c with E^Δ , the addition outperforms multiplication, while in Fig. 7f with E^δ multiplication is better.

Regarding the error bounds, the choice between E^Δ and E^δ also depends on the dataset. In Fig. 7f, choosing a relative error bound is clearly more effective than an absolute one, while in Fig. 7b the absolute bound produces better results. Generally, E^Δ is more suited for datasets having values close to zero. We should be careful at selecting E^Δ so that it does not compromise the information carried by the dataset. An example of this in Fig. 7e, where E^Δ can produce reductions close to 95%: however, as we can see from the examples in Table 4 for dataset *cmummac*, selecting $E^\Delta = 1$ would make the recovered dataset unusable. Therefore, in this case we should opt for E^δ .

5 Conclusions

In this paper, we proposed two novel lossy preprocessing techniques to improve the compression ratio of existing compressors under given error bounds by transforming the dataset before compressing it. These two methods use simple floating point arithmetic operations like addition and multiplication, as well as floating point data structure, to increase the number of common bits throughout the whole dataset. We presented the performances of these techniques by comparing their resulting CR against the one obtained without preprocessing, with lossless preprocessing, and using a similar lossy preprocessing technique [6], considering four compressors and six datasets. We plan to assess extensions of these ideas into lossless methods, as well as to achieve improvements in terms of preprocessing time.

References

- [1] G. Chiarot and C. Silvestri, “Time series compression: a survey,” 2021. [Online]. Available: <http://arxiv.org/abs/2101.08784>
- [2] R. Vestergaard, D. E. Lucani, and Q. Zhang, “A randomly accessible lossless compression scheme for time-series data,” in *IEEE INFOCOM - Conference on Computer Communications*, 2020.
- [3] E. Latyshev, “Sensor data preprocessing, feature engineering and equipment remaining lifetime forecasting for predictive maintenance,” in *DAMDID/RCDL*, 2018.
- [4] *ISO/IEC 15948:2004 Information technology — Computer graphics and image processing — Portable Network Graphics (PNG): Functional specification*, Std., 2021.
- [5] I. Batal and M. Hauskrecht, “A supervised time series feature extraction technique using dct and dwt,” in *International Conference on Machine Learning and Applications*, 2009.
- [6] J. D. e. a. M. Klöwer, M. Razinger, “Compressing atmospheric data into its real information content,” *Nat Comput Sci*, 2021.
- [7] J.-M. Muller, N. Brisebarre, and F. e. a. Dinechin, *Handbook of Floating-Point Arithmetic*, 2010.
- [8] *IEEE Std 754-2019 (Revision of IEEE Std 754-2008) IEEE Standard for Floating-Point Arithmetic*, Std., 2019.
- [9] A. Hurst, D. E. Lucani, and Q. Zhang, “GreedyGD : Enhanced generalized deduplication for direct analytics in IoT,” 2022, submitted to *IEEE Transactions on Industrial Informatics*.

- [10] Aarhus Kommune, “Sensordata,” 2017. [Online]. Available: <https://tinyurl.com/heeth2fd>
- [11] J. Seward, “bzip2,” 2019. [Online]. Available: <https://sourceware.org/bzip2/>
- [12] City of Chicago, “Beach water quality - automated sensors,” 2022. [Online]. Available: <https://tinyurl.com/yz5zy6a>
- [13] Y. Collet, F. Handte, I. Rosen, and R. Oclair, “LZ4-extremely fast compression,” 2011. [Online]. Available: <https://lz4.github.io/lz4/>
- [14] P. Fränti and S. Sieranoja, “K-means properties on six clustering benchmark datasets,” *Applied Intelligence*, 2018.
- [15] Facebook, “Zstandard – real-time data compression algorithm,” 2015. [Online]. Available: <https://facebook.github.io/zstd/>
- [16] H. Kaya and P. Tüfekci, “Gas turbine CO and NOx emission data set data set,” 2019. [Online]. Available: <https://tinyurl.com/5bc7yx8u>
- [17] J. M. e. a. F. De la Torre, J. Hodgins, “Tech. report cmu-ri-tr-08-22,” 2009. [Online]. Available: <http://kitchen.cs.cmu.edu/index.php>